Available online at www.sciencedirect.com
SCIENCE DIRECT
Dyes and Pigments 73 (2007) 186–194
DYES and PIGMENTS
www.elsevier.com/locate/dyepig

Photocatalytic degradation of an azo dye X6G in water: A comparative study using nanostructured indium tin oxide and titanium oxide thin films

Mohammad Hossein Habibi*, Nasrin Talebian

Department of Chemistry, University of Isfahan, Isfahan 81746-73441, Iran

Received 19 May 2005; received in revised form 11 August 2005; accepted 14 November 2005
Available online 24 January 2006

Abstract

Indium tin oxide (ITO) and titanium oxide (TiO_2) thin films were deposited on glass substrates using electron beam evaporation. Amorphous and crystalline films can be obtained at different annealing temperatures. The thin films are characterized by UV–vis, XRD spectra and AFM analysis. The degradation of X6G (C.I. Reactive Yellow 2), commonly used as textile dye, can be photocatalyzed by ITO and TiO_2 thin films. The degradation can be completed in the order of minutes at optimal operational parameters. Using advanced oxidation processes (AOPs) and comparison between photoactivity of both films reveal that, indium tin oxide can be used as a suitable alternative to TiO_2 thin films for water treatment.
© 2005 Elsevier Ltd. All rights reserved.

Keywords: ITO thin film; TiO_2 thin film; Photodegradation; Azo dye; Nanostructure

1. Introduction

Azo dyes are the largest group of the dyes used for dyeing cotton fabrics in the industry [1]. Cotton is the most widely used fabric among all textile materials, hence azo dyes are discharged frequently and in large quantities into the environment. The term azo dye is applied to synthetic organic colorants that are characterized by a nitrogen-to-nitrogen double bond [2]. Due to azo dyes' poor exhaustion properties as much as 30% of the initial dye applied remains unfixed and end up in effluents. A necessary criterion for the use these dyes is that they must be highly stable in light and during washing. They must also be resistant to microbial attack. Therefore, they are not readily degradable and are typically not removed from water by conventional chemical wastewater treatment systems. In the past mainly chemical coagulation followed by activated sludge process was adopted to treat textile wastewaters. However, azo dyes due to their hydrophilic property are not removed by chemical coagulation. In general, physicochemical methods (coagulation and flocculation) produce large amounts of sludge which pose handling and disposal problems. On the other hand, due to the electron withdrawing nature of the azo bonds, they are not susceptible to aerobic oxidative catabolism [3] and hence are not removed in aerobic processes. Removing color from wastes is often more important than other colorless organic substances, because the presence of small amounts of dyes (below 1 ppm) is clearly visible and influences the water environment considerably. Therefore, it is necessary to find an effective method of wastewater treatment in order to remove color from textile effluents. In recent years an alternative to conventional methods, is ''advanced oxidation processes'' (AOPs), based on the chemical, photochemical and photocatalytic production of hydroxyl radicals ($^{\bullet}OH$), which act as strong oxidizing agents, which have emerged as a promising technology for

* Corresponding author. Tel.: +98 311 793 2401; fax: +98 311 668 0066/ +98 311 668 7396.
E-mail addresses: habibi@sci.ui.ac.ir, habibi@chem.ui.ac.ir (M.H. Habibi).

0143-7208/$ - see front matter © 2005 Elsevier Ltd. All rights reserved.
doi:10.1016/j.dyepig.2005.11.006

the degradation of organic pollutants. AOPs include heterogeneous photocatalytic systems such as a combination of large band gap semiconductor particles (TiO_2, ZnO, etc.), either dispersed in slurries or immobilized on films and UV light [4–8]. The advanced oxidation processes are costly in terms of installation, operation and maintenance but decolorization of azo dyes is achieved with the cleavage of the azo bond, thus rendering the dye colorless, with the formation of corresponding aromatic amines, which can be toxic and carcinogenic [9]. Because of unique properties, a large number of semiconductor oxide films have been investigated during the past 60 years; among these titanium dioxide (TiO_2) has gained much attention because of the strong photocatalytic abilities to purify pollutants in air and water under UV irradiation [10,11]. However, In_2O_3:SnO_2 (known as indium tin oxide or ITO) films are used as transparent electrodes in flat panel displays and solar cell, surface heaters for automobile windows, camera lenses, photoelectrodes, storage-type cathode ray tubes, electrochromic devices, liquid crystal displays, electroluminescent devices, biological devices as well as transparent heat reflecting window material for building [12–18]. So far, there is little work done on ITO films used as photocatalyst. Due to the wide range of applications of ITO transparent conductive films, various techniques for the growth of these films have been intensively investigated, such as reactive thermal evaporation deposition [19], magnetron sputtering [20], electron beam evaporation [21], spray pyrolysis [22], chemical vapor deposition [23], vacuum evaporation [24], ion-assisted deposition techniques [25], electroless chemical growth techniques [26], sol-gel technique [27], and laser-assisted deposition techniques [28].

In this study, thin films of indium tin oxide and titanium oxide have been prepared on glass using an electron beam evaporation technique and the photocatalytic properties of both films toward Light Yellow X6G (C.I. Reactive Yellow 2) degradation are investigated and compared. We examined the effects of some parameters such as film thickness, dye concentration, solution pH, the presence of H_2O_2 and ethanol on the photodegradation rate.

2. Experimental

2.1. Catalysts preparation

An e-beam evaporation system was used for film deposition which is one of the most versatile techniques for the deposition of transparent conductors. Compared with other deposition techniques, the e-beam evaporation process produces films with higher purity and better-controlled composition. It also provides the films with greater adhesive strength and homogeneity and permits better control of the layer thickness. The glass substrates were first cleaned in propanol and methanol solutions in an ultrasonic bath for 10 min. The substrates were then rinsed thoroughly in deionised water and dried in a high purity N_2 gas stream just before they were loaded into the system for film deposition. ITO and TiO_2 thin films were deposited on glass substrates, whose temperature was maintained at 25 °C during the deposition process. The proportion of indium oxide to tin oxide in the coating source is typically 90:10 by mass. The thickness of the deposited films was controlled using a quartz crystal thickness monitor, resulting in film thicknesses that varied in the range of 50–300 nm.

2.2. Catalysts characterization

Surface roughness and morphologies of TiO_2 and ITO thin films were evaluated by atomic force microscopy. The X-ray diffraction (XRD) patterns obtained on a Philips D8 Advanced Bruker X-ray diffractometer using Cu K_α radiation at a scan rate of $0.03^\circ\ 2\theta\ s^{-1}$ were used to determine the identity of many phases present and their crystallite size. The accelerating voltage and the applied current were 40 kV and 35 mA, respectively. The crystallite size was calculated by X-ray line broadening analysis by Scherrer formula. UV–vis spectra of films were obtained using a UV–vis spectrophotometer (Cary 500 Scan Spectrophotometers, Varian).

2.3. Photocatalytic activity measurements

A high surface area of nanocrystalline TiO_2 and ITO thin films was prepared on microscopy glass slides. To evaluate the catalytic activity, the photodegradation of a well-known organic azo dye X6G (C.I. Reactive Yellow 2), is investigated as a simple model compound, Fig. 1, under UV irradiation. Photocatalytic experiments were carried out in air at ambient temperature by immersing samples of 15 cm^2 into 40 ml of different concentration aqueous X6G solutions. The solution was stirred continuously. The UV light (three 8 W mercury lamps) was irradiated perpendicularly to the surface of the films and the distance between the UV source and the film was 5 cm. The change of X6G concentration in accordance with the irradiation time was measured using Cary 500 Scan Spectrophotometers, Varian.

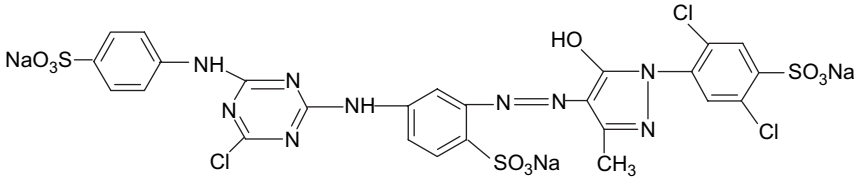

Fig. 1. Light Yellow X6G (C.I. Reactive Yellow 2).

3. Results and discussion

3.1. Characterizations of thin films

Fig. 2 shows the UV–vis absorption spectra of TiO_2 (A) and ITO (B) films, annealed at 350 °C (a), 450 °C (b) and 550 °C (c). It can be seen from Fig. 2 that the transmittance of films at 550 °C is >90% over the entire visible light spectral region. The fast decrease below 380 nm is due to absorption of light caused by the excitation of electrons from the valence band to the conduction band of both metal oxides. The oscillation of the curves between 800 and 380 nm is due to the interference between the film and the glass substrate. Compared with the transmittance spectra of TiO_2 film, the absorption edge of ITO films shows a slight pseudo-blue shift. During annealing, different temperature influenced the crystalline particle size and then influenced the absorption edge of the thin film. With smaller particle size, the electron confined in the nanomaterial exhibits different behaviors from that in the bulk materials. The properties of the electrons in small particles should be dependent upon the crystallite size and the shape due to quantized motion of the electron and hole in a confined space. As a result of the confinement, the band gap increases and the band edges shift [5]. The smaller particle the size, the larger is the blue shift; ITO film contains smaller particles, and a quantum size effect appears, resulting in a more pseudo-blue shift of the absorption edge. According to [29], the absorption coefficient α can be expressed as the following:

$$\alpha^{-1} = d\ln(1/T) \tag{1}$$

where T is the transmittance, and d is the thickness of the film. The absorption coefficient can be determined by $\alpha^n = C(h\nu - E_g)$, where n depends on the type of electron transition. In case of allowed direct and indirect transition semiconductor n is 2 and 1/2, respectively [30,31]. The linear nature of the plots of $(\alpha h\nu)^{1/2}$ for ITO and of $(\alpha h\nu)^2$ for TiO_2 thin films above the absorption edge indicates that the fundamental optical transitions in these films are indirect and direct, respectively. The values of $(\alpha h\nu)^n$ for films annealed at different temperatures are plotted vs. the photon energy (not shown

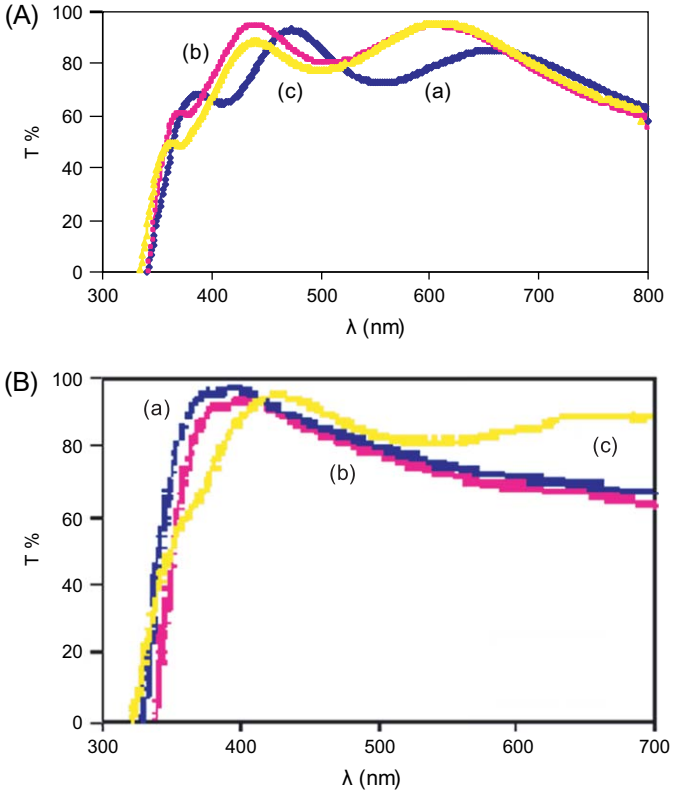

Fig. 2. UV–vis spectra of TiO_2 films (A) and ITO films (B) of 350 nm thickness annealed at 350 °C (a), 450 °C (b) and 550 °C (c).

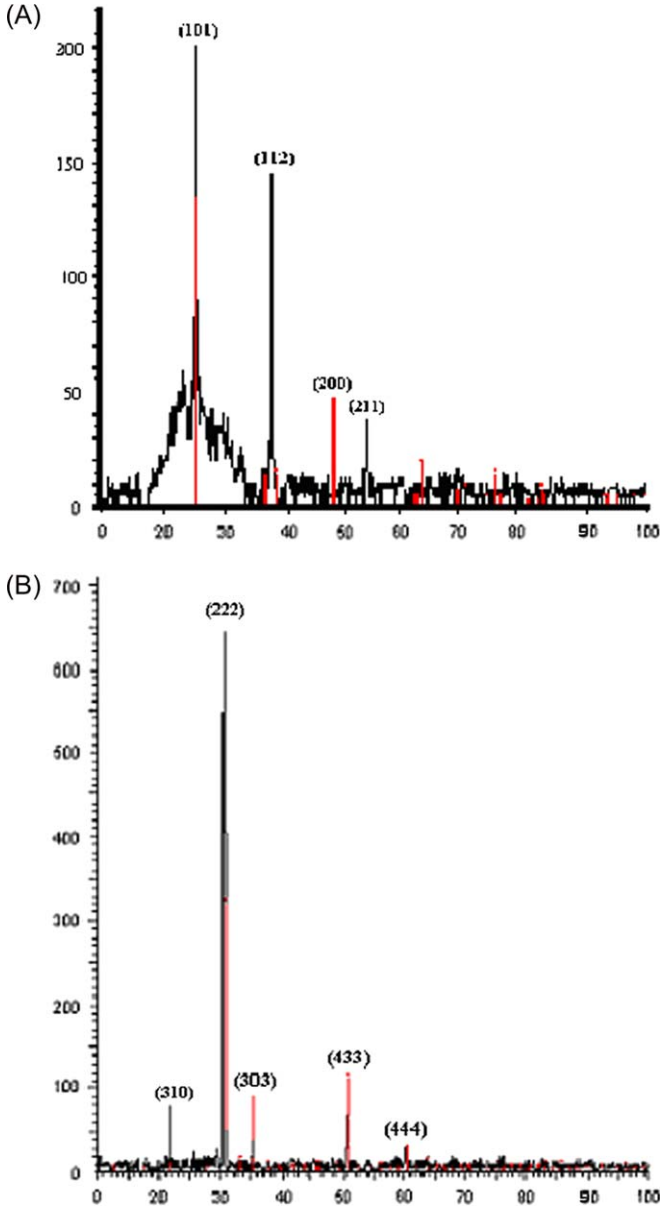

Fig. 3. (A) XRD pattern for TiO_2 thin film and (B) for ITO thin film on glass annealed at 550 °C, thickness 300 nm.

here). Extrapolating the linear region towards the $h\nu$ axis gives the effective direct transition energies for TiO_2 thin film, 3.59 eV and indirect transition energies for ITO thin film, 3.67 eV (both having 300 nm thickness), respectively.

Fig. 3(A) and (B) shows XRD patterns of TiO_2 and ITO films, deposited on glass and heat-treated at 550 °C. At 450–550 °C, TiO_2 film exhibits anatase phase structure, preferential orientation in (101) and at 550 °C, ITO film shows cubic lattice crystal structure, preferential orientation in (222). The average crystallite size of TiO_2 and ITO films annealed at 550 °C, ca. 45 and 36 nm, respectively, was calculated using the line broadening methods and the equation proposed by Scherrer [32].

Fig. 4 shows two-dimensional (a–d) and three-dimensional (e–h) AFM images of the TiO_2 (A, C) and ITO (B, D) thin films deposited on glass at 450 °C (a, c) and 550 °C (b, d). The surface morphologies and roughness of TiO_2 and ITO films are obviously different. However, both particle size and roughness of thin films are changed with annealing temperature. Fig. 4(A)(b) and (B)(d) shows that TiO_2 and ITO films annealed at 550 °C are composed of particles of about 50 and 34 nm diameters, respectively, which are nearly in agreement with those obtained from XRD spectra. In addition to particle diameter, AFM image analysis also gives the values of surface roughness. The root mean square roughness values (R_{rms}) of TiO_2 and ITO are 1.23 and 16.4 nm at 500 °C, respectively. Fig. 4(C)(f) and (D)(h) also shows that the surface morphology of ITO film is rougher than that of TiO_2 film. ITO film contains obvious pore structures between particles; hence the roughness and R_{rms} value of ITO films at 550 °C are larger than that of TiO_2 film at 550 °C.

3.2. Photocatalytic activity

The loss in absorbance at λ_{max} of X6G (406 nm) was followed during the photodegradation reaction as a function of irradiation time. The color of X6G solution changes from yellow to colorless with increasing irradiation time which indicates that there must be some chemical reaction occurring. No significant color removal was observed in the test experiments, i.e. in the presence of UV illumination (without catalysts) and in the presence of thin film catalysts (in the dark). The apparent rate constant and degradation rate of ITO film are greater than those of TiO_2 film. Characterization results of AFM, UV–vis and XRD spectra can explain the enhancement in photocatalytic activity. Firstly, AFM results show that the particle size in ITO thin films is smaller in TiO_2 films. Therefore, ITO thin films possess larger surface area. Under

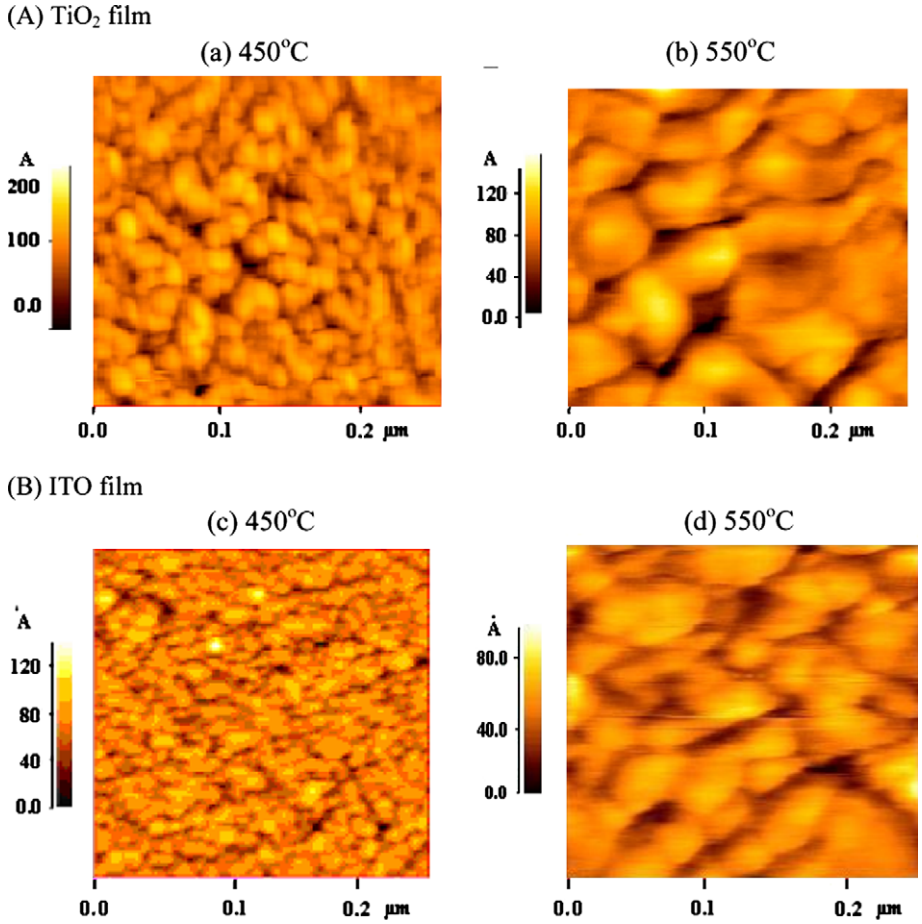

Fig. 4. Two-dimensional (a–d) and three-dimensional (e–h) AFM images of the TiO_2 (A, C) and ITO (B, D) thin films deposited on glass at (a) 450 °C and (b) 550 °C.

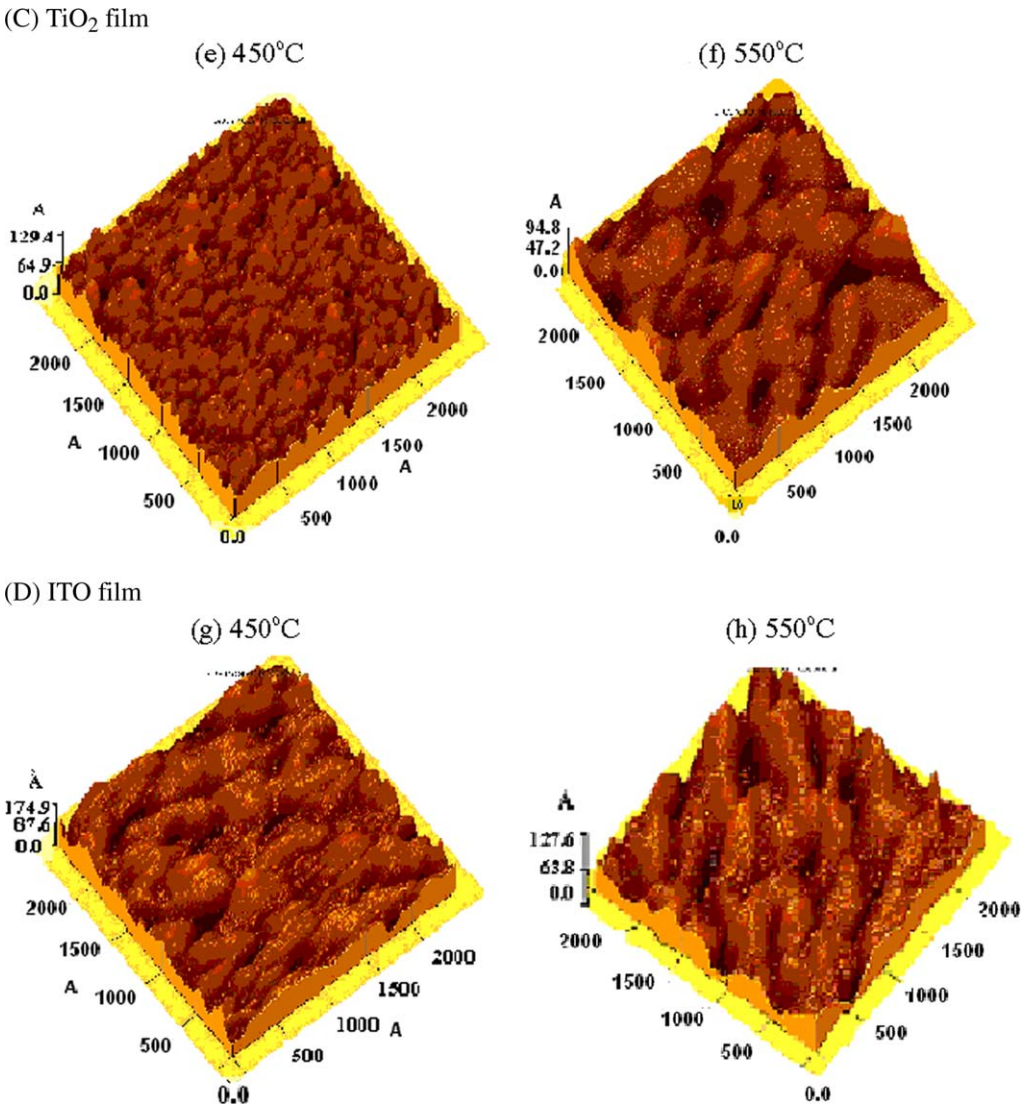

Fig. 4. (continued).

the experimental conditions used, the photocatalytic curves follow first-order reaction kinetics. Generally, the photodegradation rates of chemical compounds on semiconductor surfaces follow the Langmuir–Hinshelwood model [5,33–35].

$$R = \frac{dC}{dt} = k_r\theta = k_r KC/(1+KC) \quad (2)$$

where k_r is the reaction rate constant, K is the adsorption coefficient of the reactant, and C is the reactant concentration. The reaction rate R is proportional to the surface coverage θ; hence a high coverage θ or a large adsorption constant K would result in a high photocatalytic activity. Secondly, UV–vis spectra show that the absorption edge of ITO films is at a shorter wavelength range than that of TiO_2 film. This is because ITO films contain smaller crystallites of slightly higher band gap energy and a stronger oxidation power. XRD measurements further confirm that the crystallite size of ITO films is smaller than that of TiO_2 films. All these factors can enhance the photocatalytic activity of ITO thin films.

3.3. Factors affecting color removal

3.3.1. Effect of dye concentration

Fig. 5(A) and (B) shows a typical time-dependent UV–vis spectrum of X6G solution during photoirradiation on ITO and TiO_2 thin films, respectively. The spectrum of X6G in the visible region exhibits a main band with a maximum at 406 nm. The absorption peaks, corresponding to color of dye at $\lambda_{max} = 406$ and another, corresponding to Π–Π^* transition of aromatic rings of dye at 265 nm were diminished and finally disappeared under reaction which indicated that the dye had been degraded completely. No new absorption bands appear in the visible or ultraviolet regions. As indicated by the absorbance at 406 nm, the X6G dye was decolorized by >90% within the first 60 s at pH 1.25. However, the peak at 265 nm slightly changed within the same period of time. These results indicate that the fast decolorization of the dye was followed by a much slower mineralization of intermediates formed subsequently.

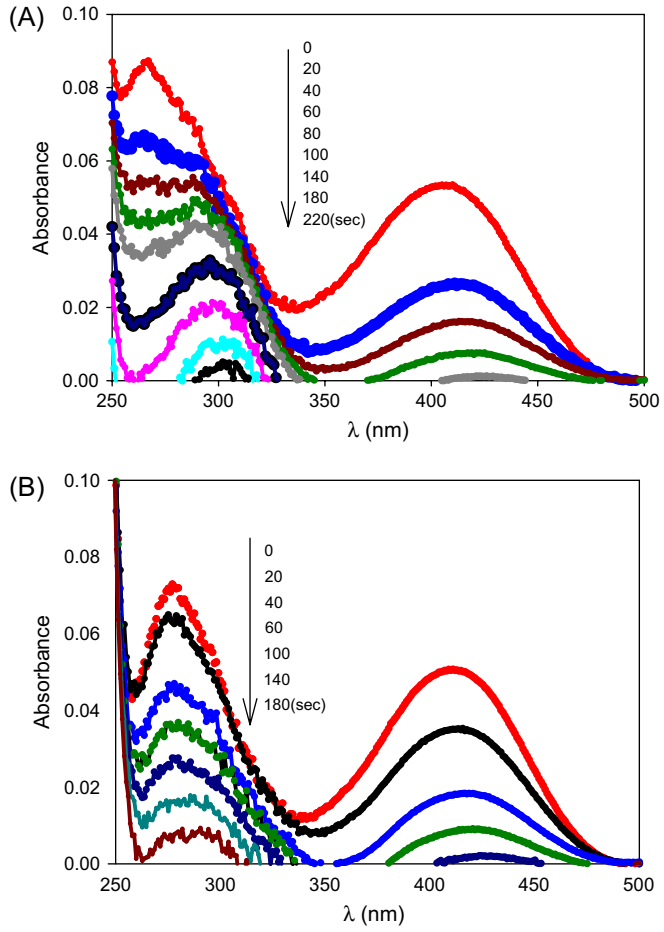

Fig. 5. Time-dependent UV–vis spectrum of X6G solution during photoirradiation on (A) TiO_2 and (B) ITO thin films; pH, 1.03; film thickness, 300 nm; dye concentration, 1×10^{-6} mol l^{-1}.

In Eq. (2) when C is very small, the KC product is negligible with respect to unity so that Eq. (2) describes first-order kinetics. The integration of Eq. (2) with the limit condition at the start of irradiation, $t = 0$, the concentration is the initial one, $C = C_0$, gives

$$\ln(C/C_0) = kt \tag{3}$$

where k is the apparent first-order reaction constant. Kinetic parameters resulting from the application of Eq. (3), are reported for different dye concentrations at pH = 1.03 on ITO and TiO_2 thin films in Table 1. The observed results in Table 1 reveal that the initial dye concentration influences the rate of degradation of the dye. The major portion of degradation occurs in the region near to the irradiated side (termed as reaction zone) where the irradiation intensity is much higher than in the other side [36]. Thus at higher dye concentration, degradation decreases at sufficiently long distances from the light source or the reaction zone due to the retardation in the penetration of light. Hence, it is concluded that as initial concentration of the dye increases, the requirement of catalyst surface needed for the degradation also increases [37]. It is important to note that for dye concentrations below 50 mg/l,

Table 1
Effect of dye concentrations on photodegradation rate of X6G

Dye concentration ($\times 10^{-6}$ mol l^{-1})	ITO Rate constant (min^{-1})	TiO_2 Rate constant (min^{-1})
1	2.94	2.59
2	1.24	0.73
4	0.45	0.42
6	0.38	0.30
8	0.29	0.21
10	0.17	0.11
12	0.09	0.06

pH 1.03, film thickness, 300 nm.

which are typically observed at wastewaters, complete degradation of X6G takes place in the order of minutes for acidic medium (Fig. 6).

3.3.2. Effect of pH

Despite the large number of accurate studies, the effect of solution pH during photocatalytic process is still not clear. The efficiencies of photocatalytic processes strongly depend upon the pH of the reaction solution. It was due to the amphoteric behavior of semiconductor ITO and TiO_2. The surface charge property of ITO and TiO_2 thin films changes with the change of solution pH. For nanosized TiO_2, the pH_{zpc} (zero point charge) is known to be 5.1 [38], so that the surface is positively or negatively charged at low or high pH, respectively. This behavior can be expected to primarily influence the adsorption of the dye on the catalyst, thus affecting the overall photocatalytic process. In the case of sulfonated dyes [39,40], a model has been proposed to account for the dramatic role played by pH in determining the critical step of the

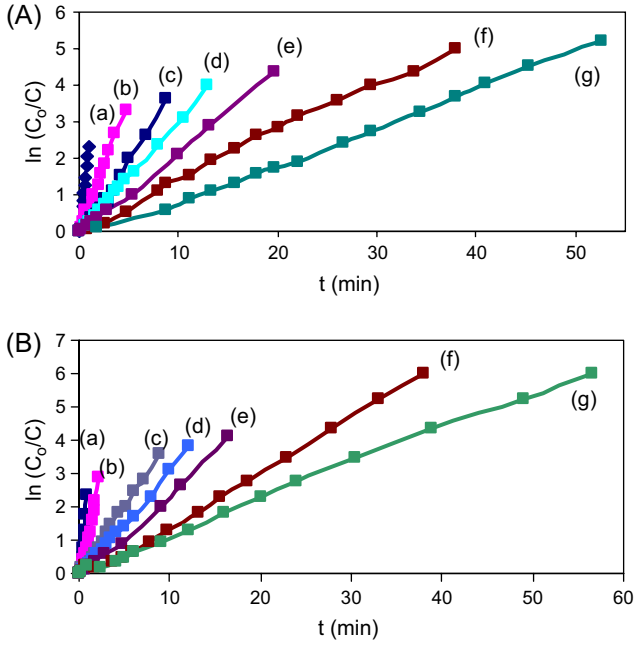

Fig. 6. Effect of dye concentrations on photodegradation rate of X6G using (A) TiO_2 thin film and (B) ITO thin film; pH, 1.03; film thickness, 300 nm; (a)–(g) dye concentration $1–12 \times 10^{-6}$ mol l^{-1}.

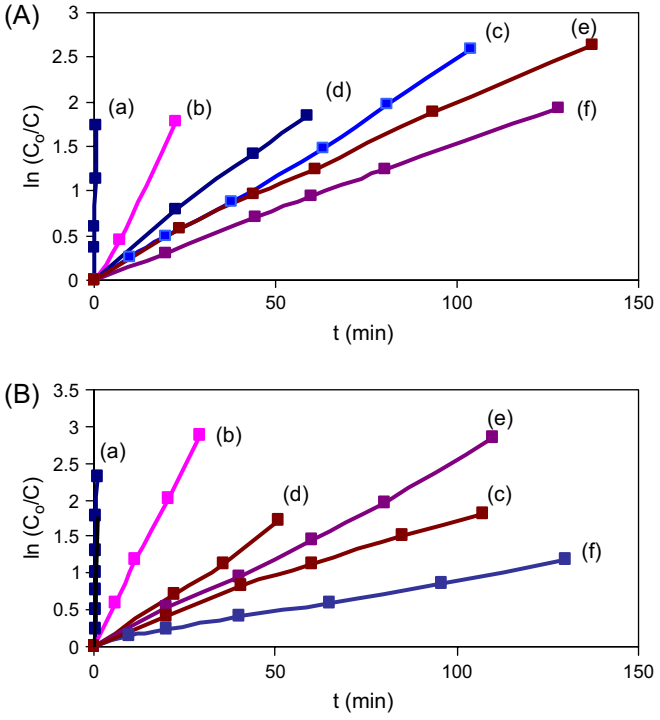

Fig. 7. pH dependence of photodegradation of X6G dye using (A) TiO_2 thin film and (B) ITO thin film. pH: (a) 1.03, (b) 2.34, (c) 4.52, (d) 6.12, (e) 7.68, and (f) 9.75; film thickness, 300 nm; dye concentration, 1×10^{-6} mol l^{-1}.

decomposition. The description considers the charge status of both the target substrate and the catalyst surface by applying a simple electrostatic reasoning. Accordingly, the increase of decolorizing recorded at acid pH was attributed to strong dye adsorption, through the deprotonated $-SO_3^-$ moiety, on the catalyst. This favorable interaction would enhance the encounter probability of nascent $^{\bullet}OH$ radicals with the organic dye. As opposed, at alkaline pH, the columbic repulsion arising between $-SO_3^-$ and the negative oxide surface would make the dye access to the catalyst a diffusion-controlled process. In this case, the $^{\bullet}OH$ radicals generated at the catalyst surface would hardly attack the target molecule. Consequently, a comparatively slower decomposition rate was measured. The same trends were observed for ITO thin film. The results of the present work for X6G are in good agreement with this model. For ITO and TiO_2 thin films, the highest percentage of dye decolorizing was actually recorded at pH 1.03 (Fig. 7, Table 2).

3.3.3. Effect of film thickness

It is seen from Fig. 8 and Table 3 that decomposition rate constants depend on the film thickness. As expected the rate constants increase with increasing film thickness which is attributed to two factors: (a) increase in amount of semiconductor dioxide to participate in the photocatalytic reaction, and (b) increase in the charge carrier concentrations of TiO_2 and ITO thin films through crystallinity improvement. However, a limiting value can be observed at thick films due to: (a) aggregation of TiO_2 and ITO particles in the interior region of thick films, causing a decrease in the number of surface active sites and (b) increase in opacity and light scattering leading to a decrease in the passage of irradiation through the film.

Table 2
Effect of pH solution on degradation rate of X6G

pH	ITO Rate constant (min^{-1})	TiO_2 Rate constant (min^{-1})
1.03	2.941	2.593
2.34	0.098	0.076
3.12	0.017	0.025
4.52	0.032	0.029
7.68	0.022	0.019
9.75	0.013	0.015

Dye concentration, 1×10^{-6} mol l^{-1}; film thickness, 300 nm.

3.3.4. Effect of hydrogen peroxide

The effect of the addition of H_2O_2 on the decolorization of azo dye was studied at different hydrogen peroxide concentrations. Results are given in Fig. 9. The decolorization rate of X6G increased with increasing H_2O_2 concentration up to 8 mmol l^{-1}, but above it, the degradation rate decreased. The higher constant rates after the addition of peroxide were attributed to the increase in the concentration of hydroxyl radical. According to Eq. (4), at low concentration, hydrogen peroxide inhibits the electron–hole recombination as the better electron acceptor than molecular oxygen [41,42].

On the other hand, hydrogen peroxide may be split photocatalytically by UV irradiation [43,44] to produce hydroxyl radical directly, (Eq. (5)). But at high concentration, H_2O_2 is a powerful $^{\bullet}OH$ scavenger (Eq. (6)) [41,45].

$$e_{CB}^- + H_2O_2 \rightarrow OH^- + {}^{\bullet}OH \quad (4)$$

$$H_2O_2 + h\nu \rightarrow 2\,{}^{\bullet}OH \quad (5)$$

$$H_2O_2 + {}^{\bullet}OH \rightarrow HO_2^{\bullet} + H_2O \quad (6)$$

Furthermore, H_2O_2 can be adsorbed onto semiconductor particles to modify their surfaces and subsequently decrease its catalytic activity [46]. Therefore, the proper amount of hydrogen peroxide could accelerate the photodegradation of X6G dye.

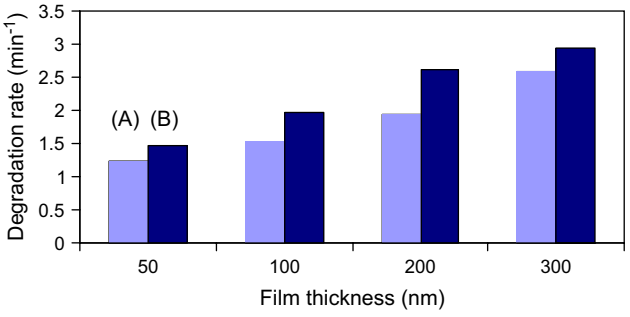

Fig. 8. The photodegradation rate variation with film thickness: (A) TiO_2 and (B) ITO films; pH, 1.03; dye concentration, 1×10^{-6} mol l^{-1}.

Table 3
Effect of film thickness on degradation rate of X6G

Film thickness	ITO Rate constant (min^{-1})	TiO_2 Rate constant (min^{-1})
50	1.46	1.25
100	1.98	1.54
200	2.62	1.95
300	2.94	2.59

Dye concentration, 1×10^{-6} mol l^{-1}, pH 1.03.

3.3.5. *Effect of ethanol*

The inhibitive influence of ethanol, commonly used to quench hydroxyl radicals, provides information on reactive species involved in the reaction. According to the previous literature [47,48], alcohols such as ethanol, are commonly used to quench hydroxyl radicals. The rate constant of reaction between hydroxyl radical and ethanol is 1.9×10^9 M^{-1} s^{-1} [42]. It was observed that small amounts of ethanol inhibited the photodegradation of X6G which means that, hydroxyl radicals play a major role in photocatalytic process. The decolorization rate decreases with an increase in the amount of ethanol (for example in the presence of 1% (v/v) ethanol, 0.005 and 0.01 min^{-1} for TiO_2 and ITO thin films, respectively).

4. Conclusion

Effective degradation of azo dyes is possible by photocatalysis in the presence of ITO and TiO_2 thin films prepared by e-beam evaporation technique and UV light. The thin films were characterized by XRD, AFM, and UV–vis. The photocatalytic activity of ITO thin films at 500 °C is obviously higher than those of TiO_2 thin films. This is attributed to the fact that ITO thin film is composed of smaller particles. ITO thin films with higher surface area and roughness are also beneficial to the enhancement of photocatalytic activity. Complete color removal was achieved at acidic pH and low concentration of X6G dye. The kinetics of the photocatalytic process follows a Langmuir–Hinshelwood model and depends on several factors such as, dye concentration, film thicknesses, pH solution and the addition of hydrogen peroxide and ethanol. The photodegradation of X6G was enhanced by the addition of proper amount of hydrogen peroxide, but it was inhibited by ethanol. From the inhibitive effect of ethanol it was detected that hydroxyl radicals played a significant role in the photodegradation of dye. Comparison between photoactivity of both thin films reveals that indium tin oxide can be used as a suitable alternative to TiO_2 thin films for water treatment.

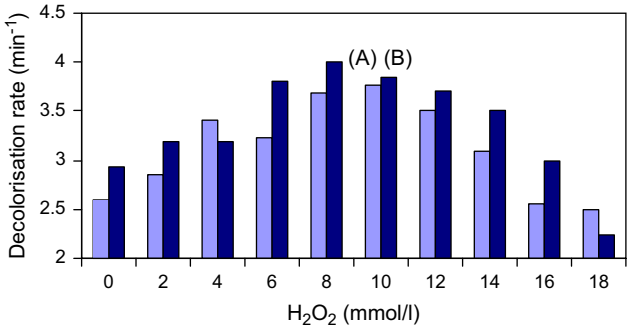

Fig. 9. Effect of H_2O_2 on decolorization rate of X6G dye: (A) TiO_2 and (B) ITO thin films of thickness 300 nm; dye concentration, 1×10^{-6} mol l^{-1}; pH, 1.03.

Acknowledgements

We are grateful to Isfahan University Graduate School for financial support of this work.

References

[1] Zhang C, Fu C, Bishop L, Kupferle M, FitzGerald S, Jiang H, et al. Transport and biodegradation of toxic organics in biofilms. J Hazard Mater 1995;41:267–85.
[2] Chudgar RJ. Dyes, application and evolution. In: Kroschwits JI, Howe-Grant M, editors. Kirk-Othmer encyclopedia of chemical technology, vol. 3. New York: John Wiley and Sons Inc.; 1991. p. 821–75.
[3] Pagga U, Taeger K. Development of a method for adsorption of dyestuffs on activated sludge. Water Res 1994;28(5):1051–7.
[4] Legrini O, Oliveros E, Braun AM. Chem Rev 1993;93:671–8.
[5] Hoffmann MR, Martin ST, Choi W, Bahnemann DW. Chem Rev 1995;95:69–96.
[6] Ollis DF, Al-Ekabi H, editors. Photocatalytic purification and treatment of water and air. Amsterdam: Elsevier Science Publishers; 1993.
[7] Turchi CS, Ollis DF. J Catal 1990;122:178–92.
[8] Fox MA, Dulay M. Chem Rev 1993;93:341–57.
[9] Wuhrmann K, Mechsner K, Kappeler T. Investigation on rate-determining factors in the microbial reduction of azo dyes. Eur J Appl Microbiol Biotechnol 1980;9:325–38.
[10] Buechler KJ, Noble RD, Koval CA, Jacoby WA. Ind Eng Chem Res 1999;38:892–6.
[11] Konstantinou IK, Sakellarides TM, Sakkas VA, Albanis TA. Environ Sci Technol 2001;35:398–405.
[12] Meng LJ, Li CH, Zhong GZ. J Lumin 1987;39:11–7.
[13] Bellingham JR, Mackenzie AP, Philips WA. Appl Phys Lett 1991;58:2506–8.
[14] Valentini A, Quaranta F, Penza M, Rizzi FR. J Appl Phys 1993;73:1143–5.
[15] Lee CH, Huang CS. Mater Sci Eng B Solid 1994;22:223–9.
[16] Copra KL, Das SR. Thin film solar cell. New York: Plenum Press; 1983. p. 321.
[17] Hamberg I, Granqvist CG. J Appl Phys 1986;60:R123–60.
[18] Pankove JI. Display devices. In: Topics in applied physics, vol. 40. Berlin: Springer-Verlag; 1980.
[19] Christian KDJ, Shatynski SR. Thin Solid Films 1983;108:319–24.
[20] Fujinaka M, Berezin AA. Thin Solid Films 1983;101:7–10.
[21] Yao JL, Hao S, Wilkinson JS. Thin Solid Films 1990;189:227–37.
[22] Pommier R, Gril C, Maruchhi J. Thin Solid Films 1981;77:91–8.
[23] Blocher JM. Thin Solid Films 1981;1980:51–64.
[24] Nath P, Bunshah RF. Thin Solid Films 1980;69:63–8.
[25] Machet J, Guille J, Saulnier P, Robert S. Thin Solid Films 1981;80:149–55.
[26] Goyal RP, Raviendra D, Gupta BR. Phys Status Solidi A 1985;87:79–81.
[27] Yamamoto O, Sasamoto T, Inagaki M. J Mater Res 1992;7:2488–91.
[28] Dai CM, Su CS, Chuu DS. Appl Phys Lett 1990;57:1879–81.
[29] Mardare D, Tasca M, Delibas M, Rusu GI. Appl Surf Sci 2000;156:200–6.
[30] Weihtens CHL, Van Loon PAC. Thin Solid Films 1991;196:1–10.
[31] Szczyrbowski J, Dietrich A, Hoffmann H. Phys Status Solidi A 1983;78:243–50.
[32] Cullity BD. Elements of X-ray diffraction. 2nd ed. MA: Addison-Wesley; 1978. p. 102.

[33] Fujishima A, Rao TN, Tryk DA. J Photochem Photobiol 2000;C1:1–21.
[34] Fernandez A, Lassaletta G, Jimenez VM, Justo A, Gonzalez-Elipe AR, Herrmann JM, et al. Appl Catal B 1995;7:49–52.
[35] Al-Ekabi H, Serpone N. J Phys Chem 1988;92:5726–31.
[36] Zhang L, Liu CY, Ren XM. J Photochem Photobiol A 1995;85:239–45.
[37] Neppolian B, Choi HC, Sakthivel S, Arabindoo B, Murugesan V. Chemosphere 2002;46:1173–81.
[38] Yang TC-K, Wang S-F, Tsai SH-Y, Lin S-Y. Appl Catal B Environ 2001;30:293–301.
[39] Tanaka K, Padermpole K, Hisanaga T. Water Res 2000;34:327–32.
[40] Reutergardh LB, Iangphasuk M. Chemosphere 1999;35:585–96.
[41] Daneshvar N, Salari D, Khataee AR. J Photochem Photobiol A 2003;157: 111–6.
[42] Khodja AA, Sehili T, Pihichowski JF, Boule P. J Photochem Photobiol A 2001;141:231–9.
[43] Stefan MI, Bolton JR. Environ Sci Technol 1999;33:870–9.
[44] Cater SR, Stefan MI, Bolton JR, Safarzadeh-Amiri A. Environ Sci Technol 2000;34:659–65.
[45] Sauer T, Neto GC, Jose HJ, Moreira RFPM. J Photochem Photobiol A 2002;149:147–54.
[46] Malato S, Blanco J, Richter C, Braun B, Maldonado MI. Enhancement of the rate of solar photocatalytic mineralization of organic pollutants by inorganic oxidizing species. Appl Catal B Environ 1998;17:347–56.
[47] Galindo C, Jacques P, Kalt A. Chemosphere 2001;45:997–1005.
[48] Daneshvar N, Salary D, Behnasuady MA. Iran J Chem Chem Eng 2002;21:55–8.